Available online at www.sciencedirect.com
ScienceDirect
Journal of Organometallic Chemistry 692 (2007) 1997–2005
Journal of Organometallic Chemistry
www.elsevier.com/locate/jorganchem

Structure and coordinate bonding nature of the manganese–σ–borane complexes

Krishna K. Pandey *

School of Chemical Sciences, D.A. University Indore, Khandwa Road Campus, Indore 452 017, India

Received 1 November 2006; received in revised form 10 January 2007; accepted 11 January 2007
Available online 19 January 2007

Abstract

The electronic and molecular structures of the complexes [(Cp′)Mn(CO)$_2$(σ-HBcat)] (**1**), [(Cp′)Mn(CO)$_2$(σ-HBpin)] (**2**) and [(Cp′)Mn(CO)$_2$(σ-HBMe$_2$)] (**3**) (Cp′ = η^5-MeC$_5$H$_4$) have been investigated at the DFT B3LYP and BP86 levels in order to understand the structures, bonding and energetics of the interactions between a transition metal and a σ-HBR$_2$ ligand. The calculated geometries are in excellent agreement with experimental values. These results are consistent with the description of [(Cp′)Mn(CO)$_2$(η^2-HBR$_2$)] as a Mn(I) complexes in which both hydrogen and boron of the [HBR$_2$] ligands have a bonding interaction with the manganese and B–H bond character is preserved. Upon coordination of [HBR$_2$], reduction in B–H bond order of about 1/3 was calculated. The LUMO of the distorted HBR$_2$ ligand is not a pure p$_\pi$ orbital, but is predominantly a hybrid (p$_\pi$-s) from boron orbitals with some contribution from H s-orbitals. The coordination of the σ-borane ligand causes a rehybridization of the boron center. NBO analysis shows that the hybrid orbital of B–H bond obtains less 2s character and more 2p character upon coordination of borane to the manganese atom. The predominant effects of the coordination of the σ-borane ligand to manganese are the decrease in the B–H bond order and accompanying increase in the B–H bond distance. The nature of the metal–ligand interactions is quantitatively analyzed with an energy decomposition method. The [(Cp′)Mn(CO)$_2$]-[η^2-H-BR$_2$] bonding in borane complexes **1**–**3** is more than half electrostatic. Indeed the three center-two electron bond in the Mn–H–B bridge may be regarded as a "protonated π-bond". The metal-η^2-H-BR$_2$ moiety in borane complexes is, therefore, analogous to metal boryl complexes with M–B σ and π bonds with a boron atom lying in the plane defined by the metal and two R substituents.

Keywords: Manganese; Borane complexes; Density functional calculations; Structure; Bonding

1. Introduction

The synthesis, characterization, structure and reactivity of transition metal σ-complexes have attracted much attention due to their role in the oxidative addition and reductive elimination steps occurring in a wide variety of catalytic processes [1]. Since the report of the first nonclassical dihydrogen complex [2] in 1984, numerous examples of agostic bond of dihydrogen [3–11] and silane [12–20] complexes have been reported. In contrast to the large number of dihydrogen complexes and σ-silane complexes, reports on stable σ-complexes of three coordinated boranes are scarce [21–29]. Borane σ complexes of titanium, manganese and rhenium reported by Hartwig et al. are the most representative examples with coordination of the B–H bond of a neutral borane to a transition metal center [21–24]. Sabo-Etienne et al. also have reported σ-borane complexes of ruthenium [27]. Mechanistic studies have revealed that σ-borane complexes can be intermediates in catalytic hydroboration processes [30].

Theoretical calculations have also been carried out to substantiate the presence of η^2-dihydrogen [9,31–37] and η^2-silane [15,18–20,38–41] coordination to many different transition metal centers, but less attention has been paid to σ-borane complexes. Ab initio calculations have been performed for σ-borane complexes [(η^5-C$_5$H$_5$)Ti{H-B(OH)$_2$}$_2$] and [(η^5-C$_5$H$_5$)Ti{HB(H)$_2$}$_2$] [21] as well as

* Tel.: +91 7312762342; fax: +91 7312365782.
E-mail address: k_k_pandey3@rediffmail.com

0022-328X/$ - see front matter © 2007 Elsevier B.V. All rights reserved.
doi:10.1016/j.jorganchem.2007.01.015

σ-borate complexes $[(\eta^5\text{-}C_5H_5)_2Nb\{H_2B(OH)_2\}]$ [42], $[(\eta^5\text{-}C_5H_5)Nb\{H_2B(C_8H_{14})\}]$ and $[(\eta^5\text{-}C_5H_5)Nb\{H_2B(H)_2\}]$ [43].

Eisenstein et al. [21] and Lledós et al. [44] have noted that these complexes are stabilized by electron donation to the metal atom from the B–H σ orbital and back donation of electron density from the metal atom to a p_π orbital. Therefore, even if there is strong back-bonding, breaking of B-H bond should not be expected. The distortion of the borane ligand (Pyramidalization) caused by the coordination has not been considered in these studies. As pointed out by Frenking et al. [45] there is a danger in the uncritical use of frontier orbitals model to explain chemical bonding because other factors such as electrostatic interactions and Pauli repulsions may also be a significant. It has been shown that the results of a bond decomposition analysis give quantitative insight into the nature of the metal–ligand interactions [46–49].

A precise electronic description of the interactions between a metal center and the B–H bond of a neutral borane has not been reported. σ-borane complexes of transition metals raise several questions of theoretical interest. One of the most striking features of the σ-coordinated boranes is the local geometry around the boron atom. The boron atom lies in the plane defined by the metal and the two R substituents as in a boryl complexes. No explanation regarding this geometrical feature has been given.

The possible valence bond representations for Mn-HBR_2 moiety is presented in Chart 1. A main question concerns whether the bonding tends more towards the σ-bond complex **I** or to the classical oxidative addition product **II**. Structures **III** and **IV** are consistent with structure **II** with some residual B–H interaction. Structure **V** favors appreciable retention of B–H bond as in structure **I** with substantial donation of metal electron density to the borane by $Mn \rightarrow B$ back-bonding. Structure **VI** represents the hydride as bridging between the Mn and B centers with a three center-two electron bond. The three center-two electron bond in Mn–H–B bridge may be regarded as a "protonated π-bond". This description is in accord with the 3c-2e bond study of Lammertsma and Ohwada [50].

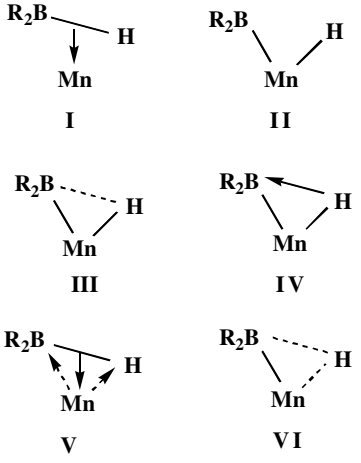

Chart 1.

In this paper, three σ-borane complexes [(Cp′)Mn-(HBcat)] (HBcat = catecholborane) (**1**), [(Cp′)Mn-(HBpin)}] (pin = pinacolborane) (**2**), $[(Cp')Mn(HBMe_2)]$ (**3**) ($Cp' = \eta^5\text{-}MeC_5H_4$) have been investigated at the DFT level using both GAUSSIAN 98 (B3LYP) and ADF-04 (BP86). The following questions are addressed in this work (i) What makes these compounds σ-borane complexes? (ii) Is the back-donation from the metal to a non-bonding p_π orbital? (iii) Why do the metal, boron and two R substituents lie in one plane? (iv) What are the relative strengths of the covalent and ionic bonding interactions that are given by the calculated attractive orbital interactions and electrostatic interactions?

2. Computational details

The calculations on all complexes have been performed using hybrid B3LYP density functional method, which uses Becke's 3-parameter nonlocal exchange functional [51] mixed with the exact (Hartree–Fock) exchange functional and Lee–Yang–Parr's nonlocal correlation function [52]. For the geometry optimizations, the basis sets [53,54] for all atoms used was the 6-31G(d). Energy calculations have been performed with basis set 6-311G(2df) for manganese and 6-311G(d) for hydrogen, boron, carbon and oxygen atoms. All equilibrium structures were optimized without any symmetry restrictions, and frequency calculations were performed to determine whether the optimized geometries were minima on the potential energy surface. The electronic structures of the $[(Cp')Mn(CO)_2(HBcat)]$ (**1**), $[(Cp')Mn(CO)_2(HBpin)]$ (**2**), $[(Cp')Mn(CO)_2(HBMe_2)]$ (**3**) and free borane ligands HBcat, HBpin, $HBMe_2$ were examined by NBO analysis [55]. The calculations were performed using the GAUSSIAN 98 program [56]. All MO pictures were made by using the MOLDEN program [57].

The geometry optimizations and bond energy decomposition analysis were performed at the nonlocal DFT level of theory using the exchange functional of Becke [58] and the correlation functional of Perdew [59] (BP86). Scalar relativistic effects have been considered using the ZORA formalism [60]. Uncontracted Slater-type orbitals (STOs) were used as basis functions for the SCF calculations [61]. Triple-ζ basis sets augmented by two sets of polarization function have been used for all the elements. The $(1s)^2$ core electrons of the boron, carbon and oxygen, $(1s2s2p)^{10}$ core electrons of manganese were treated by the frozen-core approximation [62]. An auxiliary set of s, p, d, f and g STOs was used to fit the molecular densities and to present the coulomb and exchange potentials accurately in each SCF cycle [63]. Numerical integration accuracy of INTRGRATION = 10 was used throughout. The calculations were carried out using the program package ADF-04 [64].

The bonding interactions between the fragments $[(Cp')Mn(CO)_2]$ and the $[HBR_2]$ have been analyzed using the energy decomposition scheme of ADF which is based

on the methods of Morokuma [65] and Ziegler and Rauk [66]. The bond dissociation energy ΔE between two fragments $[(Cp')Mn(CO)_2]$ and $[HBR_2]$ is partitioned into several contributions that can be identified as physically meaningful entities. First, ΔE is separated into two major components ΔE_{prep} and ΔE_{int}:

$$\Delta E = \Delta E_{prep} + \Delta E_{int} \quad (1)$$

Here, ΔE_{prep} is the energy that is necessary to promote both fragments from their equilibrium geometry and electronic ground state to the geometry and electronic state that they have in the combined molecule.

$$\Delta E_{prep} = E_{total}(\text{distorted fragments}) - E_{total}(\text{fragments in the equilibrium structure}) \quad (2)$$

ΔE_{int} is the interaction energy between the two fragments in the molecule. The interaction energy, ΔE_{int}, can be divided into three main components:

$$\Delta E_{int} = \Delta E_{elstat} + \Delta E_{Pauli} + \Delta E_{orb} \quad (3)$$

ΔE_{elstat} describes the pure coulomb interaction between two fragments and it is attractive. The second term in Eq. (3) ΔE_{Pauli} which is called exchange repulsion or Pauli repulsion, gives the repulsive interactions between the fragments that are due to the fact that two electrons with the same spin cannot occupy the same region in space. The term comprises the four-electron destabilizing interactions between occupied orbitals. ΔE_{Pauli} is calculated by enforcing the Kohn–Sham determinant of the molecule, which results from superimposing both fragments, to obey the Pauli principle through antisymmetrization and renormalization. The stabilizing orbital interaction term ΔE_{orb} is calculated in the final step of the energy analysis when the Kohn–Sham orbitals relax to their optimal form. The latter term can be further partitioned into contributions by the orbitals that belong to different irreducible representations of the point group of the system. The covalent and electrostatic character of the bond is given by the ratio $\Delta E_{elstat}/\Delta E_{orb}$ [45–49].

3. Results and discussion

3.1. Geometries

Fig. 1 shows the optimized geometries of the manganese–σ–borane complexes $[(Cp')Mn(CO)_2(\eta^2\text{-HBcat})]$ (**1**), $[(Cp')Mn(CO)_2(\eta^2\text{-HBpin})]$ (**2**), $[(Cp')Mn(CO)_2(\eta^2\text{-HBMe}_2)]$ (**3**). The optimized bond lengths and angles at B3LYP and BP86 are presented in Table 1. The optimized structures of $[(Cp')Mn(CO)_2(\eta^2\text{-HBcat})]$ and $[(Cp')Mn(CO)_2(\eta^2\text{-HBpin})]$ closely resemble that found by X-ray diffraction for **1** and **2** [24]. There is no X-ray structural data for complex **3**. The optimized geometrical data for **3** are in good agreement with X-ray diffraction for $[(Cp')Mn(CO)_2(\eta^2\text{-HBCy}_2)]$ [24]. Theoretical studies for the free borane ligands have been obtained at the same level of theory adopted for the manganese complexes. Comparisons of the free ligand to the coordinated ligand allow us to focus on the origin of the electronic and geometrical modifications that accompany coordination to the manganese atom. The B3LYP and BP86 values are very similar to each other. Geometrical data obtained using B3LYP will be discussed.

The Mn–B bond distances 2.106 Å in **1**, 2.152 Å in **2** and 2.168 Å in **3** are longer than that expected for single bond based on covalent radius predictions (2.05 Å) [67]. Using the relationship between covalent bond order and bond distance suggested by Pauling we find the calculated Mn–B distances correspond to a covalent bond order of 0.80 in **1**, 0.67 in **2**, 0.63 in **3** [68]. The B–H bond distances 1.306 Å in **1**, 1.312 Å in **2** and 1.311 Å in **3** are also longer than expected for a single bond based on covalent radius predictions (1.19 Å) and those obtained by theoretical study for the free borane ligands (1.184 Å in HBcat, 1.190 Å in HBpin and 1.204 Å in $HBMe_2$). The optimized B–H bond distances in σ-borane complexes **1**–**3** correspond to a covalent bond order of about 2/3. The B–Mn–H1 bond angles in the complexes $[(Cp')Mn(CO)_2(\eta^2\text{-HBR}_2)]$: 38.3° in **1**, 37.4° in **2** and

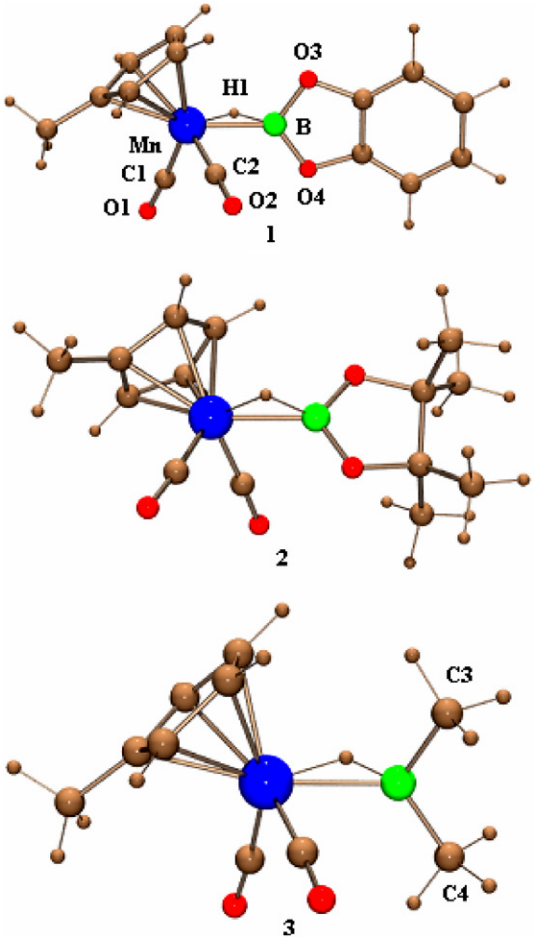

Fig. 1. Optimized geometries of the manganese–σ–borane complexes $[(Cp')Mn(CO)_2(\eta^2\text{-HBcat})]$ (**1**), $[(Cp')Mn(CO)_2(\eta^2\text{-HBpin})]$ (**2**) and $[(Cp')Mn(CO)_2(\eta^2\text{-HBMe}_2)]$ (**3**).

Table 1
Selected optimized geometrical parameters for manganese–σ–borane complexes [(Cp′)Mn(CO)$_2$(HBR$_2$)] (**1**, R$_2$ = cat; **2**, R$_2$ = pin; **3**, R = Me)[a], [(Cp′)Mn(CO)$_2$], HBcat, HBpin, HBMe$_2$ and X-ray data for **1**, **2** and **3**[b]

	[(Cp′)Mn(CO)$_2$(HBcat)]		[(Cp′)Mn(CO)$_2$(HBpin)]		[(Cp′)Mn(CO)$_2$(HBMe$_2$)]		[(Cp′)Mn(CO)$_2$]	HBcat	HBpin	HBMe2
	B3LYP (BP86)	X-ray (**1**)	B3LYP (BP86)	X-ray (**2**)	B3LYP (BP86)	X-ray (**3**[c])	B3LYP (BP86)	B3LYP (BP86)	B3LYP (BP86)	B3LYP (BP86)
Bond distances										
Mn–B	2.106(2.095)	2.083(2)	2.152(2.141)	2.149(2)	2.168(2.173)	2.187(3)				
Mn–H1	1.602(1.604)	1.57(2)	1.597(1.590)	1.53(2)	1.620(1.609)	1.49(2)				
Mn–C1	1.790(1.775)	1.788(2)	1.773(1.767)	1.776(2)	1.786(1.770)	1.777(3)	1.787(1.776)			
Mn–C2	1.779(1.772)	1.774(2)	1.786(1.775)	1.785(2)	1.774(1.769)	1.770(3)	1.784(1.775)			
B–H1	1.306(1.355)	1.29(2)	1.312(1.367)	1.31(2)	1.311(1.355)	1.24(2)		1.184(1.186)	1.190(1.194)	1.204(1.208)
B–O3	1.403(1.413)	1.404(2)	1.381(1.391)	1.376(2)				1.384(1.389)	1.367(1.373)	
B–O4	1.405(1.418)	1.413(2)	1.377(1.387)	1.376(2)				1.384(1.389)	1.367(1.373)	
C1–O1	1.158(1.164)	1.149(2)	1.163(1.169)	1.155(2)	1.159(1.170)	1.160(3)	1.161(1.169)			
C2–O2	1.161(1.165)	1.153(2)	1.159(1.166)	1.154(2)	1.164(1.167)	1.160(3)	1.162(1.169)			
B–C3					1.587(1.587)	1.590(3)				1.569(1.567)
B–C4					1.586(1.583)	1.590(3)				1.569(1.567)
Bond angles										
Mn–H1–B	92.2(89.8)		94.9(92.5)		94.9(93.9)					
Mn–B–H1	49.5(50.0)	48.6(6)	47.7(47.9)	44.7(9)	48.1(47.6)	41.1(9)				
B–Mn–H1	38.3(40.2)	38.2(6)	37.4(39.6)	37.2(8)	37.1(38.5)	33.2(7)				
C1–Mn–C2	93.0(90.5)	90.66(7)	91.5(89.7)	90.32(7)	98.2(91.6)	93.4(1)	96.4(93.9)			
O3–B–O4	110.1(109.6)	109.8(1)	112.6(112.3)	112.7(1)				111.9(112.1)	114.0(114.3)	
Mn–B–O3	126.9(127.4)	127.9(1)	119.9 (120.4)	121.6(1)		116.7(1)				
Mn–B–O4	121.3(121.9)	121.4(1)	125.7(126.3)	124.5(1)		125.1(2)				
C3–B–C4					117.2(117.5)	117.9(2)				124.3(122.2)
Mn–B–C3					119.0(118.8)	116.7(1)				
Mn–B–C4					122.6(123.0)	125.1(2)				

[a] See Fig. 1 for labeling of the atoms. Distances are in Å and angles in °.
[b] X-ray data are taken from Ref. [24].
[c] X-ray data for [(Cp′)Mn(CO)$_2$(HBCy$_2$)].

37.1° in **3** are very small and are consistent with B–H bonding. These results are consistent with [(Cp′)Mn(CO)$_2$(HBR$_2$)] being Mn(I) complexes in which both hydrogen and boron of the [HBR$_2$] ligands have a bonding interaction with the manganese preserving B–H bond character. Thus, the complexes **1**–**3** are σ-borane complexes rather than hydride-boryl complexes. Upon coordination of the borane ligand, the B–O bond distances are lengthened by 0.020 Å in HBcat, 0.012 in HBpin and the B–C bond distances are lengthened by 0.017 Å in HBMe$_2$.

3.2. Bonding analysis of manganese–σ–borane bond

We begin the analysis of the bonding in the σ-borane complexes **1**–**3** with a discussion of the conventional indices that are frequently used to characterize the bonding in molecules, that is, bond orders and atomic charges. Table 2 gives the Wiberg bond indices [69] (WBI), which provide bond orders, and the natural bond orbital (NBO) analysis. To examine the charge flow between the borane ligands [HBR$_2$] and the metal fragment [(Cp′)Mn(CO)$_2$] in the complexes, the NBO charges of the fragments in the frozen geometries of the molecules have been calculated. The results are shown in Fig. 2.

Table 2 shows that the WBI values of the Mn–B bonds of the complexes **1**–**3** are small ∼0.45. Although the Mn–H distances are short (∼1.6 Å), the WBI values of the Mn–H bonds are small (∼0.25). Upon coordination of the borane ligand, the B–H bond orders are calculated to be reduced by ∼1/3.

Table 2
Wiberg bond indices, and results of the NBO analysis in [(Cp′)Mn(CO)$_2$(HBR$_2$)] complexes and in free ligands

	1	**2**	**3**	HBcat	HBpin	HBMe$_2$
Wiberg bond indices						
Mn–B	0.46	0.43	0.45			
Mn–H1	0.25	0.28	0.25			
Mn–C1	1.08	1.05	1.10			
Mn–C2	1.01	1.09	1.10			
B–H	0.63	0.62	0.66	0.97	0.96	0.97
C1–O1	2.02	1.97	2.01			
C2–O2	1.99	2.01	1.96			
NBO analysis						
Mn–B bond						
Occupancy	1.53674	1.33339	1.45597			
Mn						
%	74.24	65.33	75.43			
%s	7.94	21.76	9.34			
%p	0.13	0.39	0.20			
%d	91.93	77.84	90.45			
B						
%s	29.50	27.55	15.04			
%p	78.37	72.32	84.29			
%d	0.11	0.13	0.17			
B–H bond						
Occupancy	1.65503	1.64858	1.66452	1.98454	1.98220	1.98280
B						
%	39.91	39.36	38.02	45.67	45.31	45.42
%s	21.37	20.41	19.26	44.74	39.93	32.24
%p	78.37	79.33	80.50	55.15	59.96	67.62
%d	0.26	0.26	0.24	0.11	0.11	0.14
H						
%s	100.00	100.00	100.00	100.00	100.00	100.00
Mn–H–B bond						
Occupancy	1.85422	1.84847	1.85017			
Mn (%)	9.96	9.81	9.28			
H (%)	49.72	49.89	51.59			
B (%)	33.03	32.70	31.63			
NBO charges						
Mn	0.79	0.80	0.85			
B	0.72	0.74	0.38	0.92	0.92	0.69
H	−0.04	−0.05	−0.05	−0.08	−0.09	−0.09
R$_2$	−0.88	−0.86	−0.57	−0.84	−0.83	−0.60

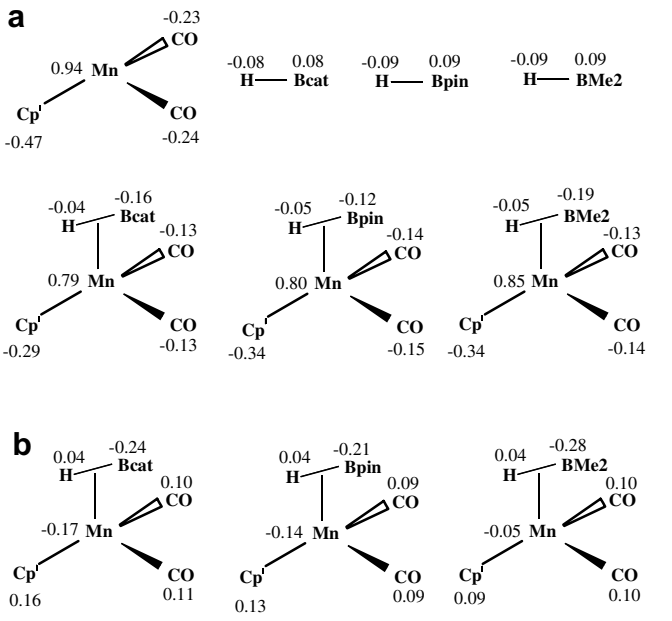

Fig. 2. (a) Calculated NBO charges for complexes **1**–**3** and its fragments; (b) changes in caused by coordination of HBR_2 to $[(Cp')Mn(CO)_2]$.

The computed charges (Fig. 2) indicate that the manganese atom always carries a positive charge, while all other groups i.e. CO, Cp′ and HBR_2 are negatively charged. More information can be revealed when the charge flows between the interacting fragments $[(Cp')Mn(CO)_2]$ and HBR_2 are compared. Fig. 2 shows the net electron transfer from the $[(Cp')Mn(CO)_2]$ fragment to borane ligands HBcat (0.20 electron), HBpin (0.17 electron) and $HBMe_2$ (0.24 electron).The back-donated electron density from the metal fragment mainly resides on boron atom (Table 2). We note that the manganese atom in complexes **1**–**3** has lesser positive charge than that in the metal fragment (Fig. 2). This is remarkable, because there is an overall charge flow in the direction $[(Cp')Mn(CO)_2] \rightarrow [HBR_2]$. It follows that the ligands CO and Cp′ donate electronic charge to manganese atom and to the borane ligand in **1**–**3**. The transfer of electron density from manganese fragment to borane ligands induces the geometrical response of pyramidalization of the HBR_2 moiety.

A more definitive picture of Mn–B, Mn–H and B–H bonding is obtained through NBO analysis of the delocalized Kohn–Sham orbitals. The characteristics of the Mn–B and M–H–B bonding orbitals are listed in Table 2. The occupancies of these orbitals are relatively low. The Mn–B bonding orbitals are polarized towards Mn, while the B–H bonding orbitals are polarized towards H. The coordination of a σ-borane ligand causes a rehybridization of the boron center. The hybrid orbital of boron along the B–H bond in the free ligand is $sp^{1.23}$ (HBcat), $sp^{1.50}$ (HBpin), $sp^{2.10}$ ($HBMe_2$) and in the borane complexes is $sp^{3.67}$ (**1**), $sp^{3.89}$ (**2**) and $sp^{4.16}$ (**3**). These results reveal that less 2s character and more 2p character goes to the B–H bond upon coordination of borane to manganese atom.

Table 3
Energy decomposition analysis of $[(Cp')Mn(CO)_2(\eta^2\text{-HBcat})]$ (**1**), $[(Cp')Mn(CO)_2(\eta^2\text{-HBpin})]$ (**2**) and $[(Cp')Mn(CO)_2(\eta^2\text{-HBMe}_2)]$ (**3**) at BP86/TZP[a]

	1	2	3
ΔE_{int}	−46.5	−44.4	−47.6
ΔE_{Pauli}	117.1	108.8	109.0
ΔE_{elstat}	−87.5	−84.6	−82.8
ΔE_{orb}[b]	−76.1	−68.6	−73.8
	(46.5%)	(44.8%)	(47.1%)
ΔE_{prep}	16.1	15.1	13.3
$\Delta E(-D_e)$	−30.4	−29.3	−34.3

[a] Energy contributions in kcal/mol.
[b] The values in parentheses are the percentage contribution to the total attractive interactions reflecting the covalent character of the bond.

The Mn–H–B bond shows a weaker Mn–H bond. The 2-center Mn–H NBO was not found. The most evident effects of the coordination of σ-borane ligand to manganese are the decrease in B–H bond order and hence increase in B–H bond distance. To quantify this information and to get a more detailed insight in to the nature of the Mn–η^2–H–BR_2 interactions, energy partitioning analysis has been performed. The results are given in Table 3.

Table 3 shows the results of the partitioning of the interaction energy ΔE_{int} of the combination of $[(Cp')Mn(CO)_2]$ and $[HBR_2]$ into the three terms ΔE_{Pauli}, ΔE_{elstat}, and ΔE_{orb}. The bonding energies of compound **1** (−30.44 kcal/mol), **2** (−29.34 kcal/mol) and **3** (−34.34 kcal/mol) are almost twice the mean value of metal-(η^2-H_2) bonding energies and larger than the experimental dissociation enthalpy for η^2-HBcat was found 25 ± 3 kcal/mol in $[(Cp')Mn(CO)_2(\eta^2\text{-HBcat})]$ [24]. We note that, for Mn–η^2–H–BR_2 bonds in the complexes **1**–**3**, the contribution of electrostatic attractions ΔE_{elstat} are greater than the orbital interactions, ΔE_{orb}. The repulsive terms ΔE_{Pauli} were largest in each case. Table 3 shows that the trends of ΔE_{Pauli} and ΔE_{orb} from complexes **1** to **3** are roughly same, while the ΔE_{elstat} values decrease for **1**–**3**. The $[(Cp')Mn(CO)_2]$-$[\eta^2$-H-$BR_2]$ bonding in borane complexes **1**–**3** is more than half electrostatic. All three complexes exhibit about 45% covalent bonding of the borane ligand to the metal fragment.

In order to visualize the Mn–B, B–H and Mn–B–H bonding, envelope plots of some relevant orbitals of $[(Cp')Mn(CO)_2(HBMe_2)]$ and the fragments $[(Cp')Mn(CO)_2]$ and $[HBR_2]$ are shown in Fig. 3. The HOMO and LUMO of the fragment $HBMe_2$ are shown in Fig. 3a and b. The LUMO of the $[(Cp')Mn(CO)_2]$ fragment shown in Fig. 3c is predominantly metal d_{z^2} orbital and the HOMO of the $[(Cp')Mn(CO)_2]$ fragment shown in Fig. 3d is predominantly metal d_π orbital. The molecular orbitals that result from interaction of these frontier orbitals of $[(Cp')Mn(CO)_2]$ with $[HBMe_2]$ are shown in Fig. 3e–g. Molecular orbital, Fig. 3e, is a well-formed Mn–H–B bond while molecular orbital, Fig. 3f, is a well-formed Mn–B bond. Fig. 3g of the $[(Cp')Mn(CO)_2(HBMe_2)]$ gives a pictorial description of the vacant π^* orbital. As mentioned earlier structure **VI**

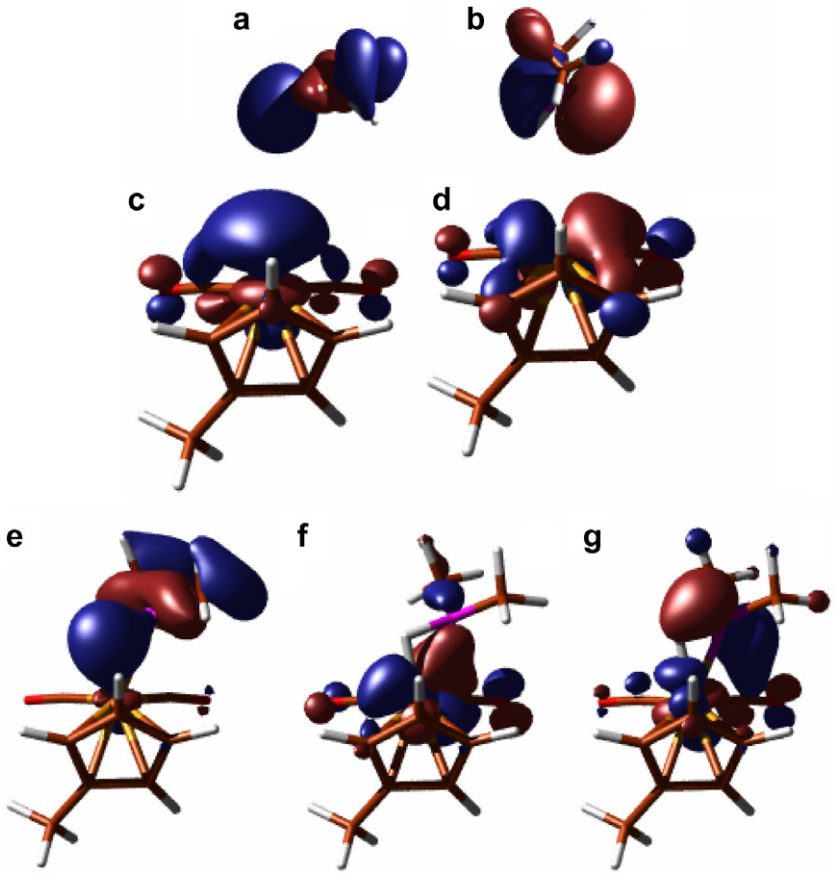

Fig. 3. Plot of some relevant orbitals of $[(Cp')Mn(CO)_2(\eta^2\text{-}HBMe_2)]$ and its fragments $[(Cp')Mn(CO)_2]$ and $[HBMe_2]$.

(Chart 1) contains a hydride that is bridging the Mn and B centers with a three center-two electron bond. The three center-two electron bonds in Mn–H–B (Fig. 3e) may be regarded as a "protonated π-bond". This description is in accord with the 3c-2e bond study of Lammertsma and Ohwada [50]. Thus, the Mn–η^2–H–BR_2 moiety in borane complexes **1**–**3** is analogous to metal boryl complexes with Mn-B σ and π bonds with the boron atom lying in the plane defined by the metal and two R substituents. This bonding description is one of the possible explanations for the planarity around the boron atom in the σ-borane complexes.

3.3. Vibrational frequencies

The vibrational wavenumbers and infrared intensities calculated at the B3LYP level of theory are presented in Table 4 for the complexes **1**, **2** and **3**. The ν_{H-B} in the free borane ligands is calculated at 2670 cm^{-1} for HBcat, at 2617 cm^{-1} for HBpin and at 2491 cm^{-1} for $HBMe_2$. Thus, a low frequency shift of 910 cm^{-1} in the case of **1**, 835 cm^{-1} in the case of **2** and 741 cm^{-1} in the case of **3** is observed for the activated Mn–(η^2–H–B) bonds. The stretching frequency in the region 1750–1782 cm^{-1} is better described as a $\nu_{(Mn-H-B)}$. These values agree reasonably well with experimental and calculated IR vibrational data for the bridging M–H–B group. The calculated vibrational frequencies, $\nu_{(CO)}$ are within 30 cm^{-1} of the experimental values.

Table 4
Selected vibrational frequencies (cm^{-1}) and infrared intensities[a] (km/mol) in $[(Cp')Mn(CO)_2(HBR_2)]$ complexes

	$\nu_{(CO)}$		$\nu_{(Mn-H-B)}$	
	Exptl	B3LYP	Exptl	B3LYP
$[(Cp')Mn(CO)_2(HBcat)]$	1937 1995	1956(888) 1999(668)	1606	1760(56)
$[(Cp')Mn(CO)_2(HBpin)]$	1921 1983	1942(846) 1992(698)	1603	1782(180)
$[(Cp')Mn(CO)_2(HBMe_2)]$	1910 1975	1937(836) 1988(652)	1592	1750(276)

[a] Intensities are in parentheses.

4. Conclusion

In the present DFT study, we investigated geometries and bonding in σ-borane complexes $[(Cp')Mn(CO)_2(HBcat)]$ (**1**), $[(Cp')Mn(CO)_2(HBpin)]$ (**2**) and $[(Cp')Mn(CO)_2(HBMe_2)]$ (**3**). The calculated geometries are in excellent agreement with experimental values. These results are consistent with a description of $[(Cp')Mn\text{-}(CO)_2(\eta^2\text{-}HBR_2)]$ as Mn(I) with both hydrogen and boron of the $[HBR_2]$

ligands bonding with the manganese while preserving B–H bond character. Upon coordination of [HBR_2], reduction in B–H bond order of approximately 34% has been observed. The LUMO of the distorted HBR_2 ligand is a predominantly boron hybrid (p_π-s) with some contributions from the H s-orbitals. The most predominant effects of the coordination of σ-borane ligand to manganese are the decrease in the B–H bond order and the accompanying increase in B–H bond distance. The bonding energies of compound **1** (−30.44 kcal/mol), **2** (−29.34 kcal/mol) and **3** (−34.34 kcal/mol) are small. For the Mn–η^2–H–BR_2 bonds in the complexes **1**–**3**, the contribution of the electrostatic attractions ΔE_{elstat} are greater than the orbital interactions, ΔE_{orb}. The repulsive term ΔE_{Pauli} always has the largest value. Thus, the [(Cp′)$Mn(CO)_2$]–[η^2–H–BR_2] bonding in borane complexes **1**–**3** is more than half electrostatic. All three complexes exhibit about 45% covalent bonding of the borane ligand to the metal fragment.

References

[1] (a) G.J. Kubas, in: J.P. Fackler (Ed.), Metal Dihydrogen and σ-Bond Complexes, Kluwer Academic/Plenum Publishers, New York, 2001; (b) G.J. Kubas, Catal. Lett. 105 (2005) 79.
[2] G.J. Kubas, R.R. Ryan, B.L. Swanson, P.J. Vergamini, H.J. Wasserman, J. Am. Chem. Soc. 106 (1984) 451.
[3] G.J. Kubas, Acc. Chem. Res. 21 (1988) 120.
[4] R.H. Crabtree, Acc. Chem. Res. 23 (1990) 95.
[5] P.G. Jessop, R.H. Morris, Coord. Chem. Rev. 121 (1992) 155.
[6] D.M. Heinekey, W.J. Oldham Jr., Chem. Rev. 93 (1993) 913.
[7] R.H. Crabtree, Angew. Chem., Int. Ed. Engl. 32 (1993) 789.
[8] M.A. Esteruelas, L.A. Oro, Chem. Rev. 98 (1998) 577.
[9] J. Tomas, A. Lledós, Y. Jean, Organometallics 17 (1998) 190.
[10] G. Frenking, N. Fröhlich, Chem. Rev. 100 (2000) 717.
[11] F. Maseras, A. Lledós, Chem. Rev. 100 (2000) 601.
[12] U. Schubert, Adv. Organomet. Chem. 30 (1990) 151.
[13] J.Y. Corey, M. Elder, J. Braddock-Wilking, Chem. Rev. 99 (1999) 175.
[14] S. Sabo-Etienne, B. Chaudret, Coord. Chem. Rev. 178 (1998) 381.
[15] F. Delpech, S. Sabo-Etienne, J.-C. Daran, B. Daran, B. Chaudret, K. Hussein, C.J. Marsden, J.-C. Barthelat, J. Am. Chem. Soc. 121 (1999) 6668.
[16] I. Atheaux, B. Donnadieu, V. Rodriguez, S. Sabo-Etienne, B. Chaudret, K. Hussein, J.-C. Barthelat, J. Am. Chem. Soc. 122 (2000) 5664.
[17] N.M. Yardy, F.R. Lemke, L. Brammer, Organometallics 20 (2001) 5670.
[18] G.I. Nikonov, Organometallics 22 (2003) 1597.
[19] D.I. Lichtenberger, Organometallics 22 (2003) 1599.
[20] (a) S.R. Dubberley, S.K. Ignatov, N.H. Rees, A.G. Razuvaev, P. Mountford, G.I. Nikonov, J. Am. Chem. Soc. 125 (2003) 642; (b) G.I. Nikonov, Adv. Organomet. Chem. 53 (2005) 217, and references therein.
[21] J.F. Hartwig, C.N. Muhoro, X. He, O. Eisenstein, R. Bosque, F. Maseras, J. Am. Chem. Soc. 118 (1996) 10936.
[22] C.N. Muhoro, J.F. Hartwig, Angew. Chem., Int. Ed. Engl. 36 (1997) 1510.
[23] C.N. Muhoro, X. He, J.F. Hartwig, J. Am. Chem. Soc. 121 (1999) 5033.
[24] S. Schlecht, J.F. Hartwig, J. Am. Chem. Soc. 122 (2000) 9435.
[25] R. Macias, N.P. Rath, L. Barton, Angew. Chem., Int. Ed. 38 (1999) 162.
[26] M. Shimoi, S. Nagai, M. Ichikawa, Y. Kawano, K. Katoh, M. Uruichi, H. Ogino, J. Am. Chem. Soc. 121 (1999) 11704.
[27] (a) V. Montiel-Palma, M. Lumbierres, B. Donnadieu, S. Sabo-Etienne, B. Chaudret, J. Am. Chem. Soc. 124 (2002) 5624; (b) S. Lachaize, K. Essalah, V. Montiel-Palma, L. Vendier, B. Chaudret, J.-C. Barthelat, S. Saba-Etienne, Organometallics 24 (2005) 2935.
[28] D. Liu, K.C. Lam, Z. Lin, Organometallics 22 (2003) 2827.
[29] W.H. Lam, S. Shimada, A.S. Batsanov, Z. Lin, T.B. Marder, J.A. Cowan, J.A.K. HcMason, G.J. McIntyre, Organometallics 22 (2003) 4557.
[30] J.F. Hartwig, C.N. Muhoro, Organometallics 19 (2000) 30.
[31] P.J. Hay, J. Am. Chem. Soc. 109 (1987) 705.
[32] J. Eckart, G.J. Kubas, J.H. Hall, P.J. Hay, C.M. Boyle, J. Am. Chem. Soc. 112 (1990) 2324.
[33] G.R. Haynes, R.L. Martin, P.J. Hay, J. Am. Chem. Soc. 114 (1992) 28.
[34] S. Dapprich, G. Frenking, Angew. Chem., Int. Ed. Engl. 34 (1995) 354.
[35] J. Li, T. Ziegler, Organometallics 15 (1996) 3844.
[36] J. Li, R.M. Dickson, T. Ziegler, J. Am. Chem. Soc. 117 (1995) 11482.
[37] A. Jarid, M. Moreno, A. Lledós, J.M. Lluch, J. Bertrán, J. Am. Chem. Soc. 117 (1995) 1069.
[38] M.F. Fan, G. Jia, Z. Lin, Z.J. Am. Chem. Soc. 118 (1996) 9915.
[39] M.F. Fan, Z. Lin, Organometallics 16 (1997) 494.
[40] F. Maseras, A. Lledós, Organometallics 15 (1996) 1216.
[41] K. Hussein, C.J. Marsden, J.-C. Barthelat, V. Rodriguez, S. Conejero, S. Saba-Etienne, B. Donnadieu, B. Chaudret, Chem. Commun. (1999) 1315.
[42] K.K. Pandey, Inorg. Chem. 40 (2001) 5092.
[43] A. Antinolo, F. Carrillo-Hermosilla, J. Fernandez-Baeza, S. Garcia-Yuste, A. Otero, A.M. Rodriguez, J. Sanchez-Prada, E. Villasenor, R. Gelabert, M. Moreno, J.M. Lluch, A. Lledós, Organometallics 19 (2000) 3654.
[44] I. Demachy, M.A. Esteruelas, Y. Jean, A. Lledós, F. Maseras, L.A. Oro, C. Valero, F. Volatron, J. Am. Chem. Soc. 118 (1996) 8388.
[45] A. Diefenbach, M.B. Bickelhaupt, G. Frenking, J. Am. Chem. Soc. 122 (2000) 6449.
[46] J. Uddin, G. Frenking, J. Am. Chem. Soc. 123 (2001) 1683.
[47] K.K. Pandey, M. Lein, G. Frenking, J. Am. Chem. Soc. 125 (2003) 1660.
[48] K.K. Pandey, Inorg. Chem. 42 (2003) 6764.
[49] G. Frenking, K. Wichmann, N. Froehlich, C. Loschen, M. Lein, J. Frunzke, V.M. Rayon, Coord. Chem. Rev. 238–239 (2003) 55.
[50] K. Lammertsma, T. Ohwada, J. Am. Chem. Soc. 118 (1996) 7247.
[51] C. Lee, W. Yang, R.G. Parr, Phys. Rev. B 37 (1988) 785.
[52] D. Becke, J. Chem. Phys. 98 (1993) 5648.
[53] K. Raghavachari, J.S. Binkley, R. Seeger, J.A. Pople, J. Chem. Phys. 72 (1980) 650.
[54] A.D. McClean, G.S. Chandler, J. Chem. Phys. 72 (1980) 5639.
[55] A.E. Reed, L.A. Curtiss, F. Weinhold, Chem. Rev. 88 (1988) 899.
[56] M.J. Frisch, G.W. Trucks, H.B. Schlegel, G.E. Scuseria, M.A. Robb, J.R. Cheeseman, B.G. Zarzewski, J.A. Montgomery, R.E. Startmann, J.C. Burant, S. Dapprich, J.M. Millam, A.D. Daniels, K.N. Kudin, M.C. Straiin, O. Farkas, J. Tomasi, V. Barone, M. Cossi, R. Cammi, B. Mennucci, C. Pomelli, C. Adamo, S. Clifford, J. Ochteriski, G.A. Petersson, P.Y. Ayala, Q. Cui, K. Morokuma, P. Salvador, J.J. Dannenberg, D.K. Malick, A.D. Rabuck, K. Raghavachari, J.B. Foresman, J. Cioslowski, J.V. Ortiz, A.G. Baboul, B.B. Stefanov, G. Liu, A. Liashenko, P. Piskorz, I. Komaromi, R. Gomperts, R.L. Martin, D.J. fox, T. Keith, M.A. Al-Laham, C.Y. Peng, A. Nanayakkara, M. Challacombe, P.M.W. Gill, B.G. Johnson, W. Chen, M.W. Wong, J.L. Andres, C. Gonzalez, M. Head-Gordon, E.S. Replogle, J.A. Pople, GAUSSIAN 98, Gussain, Inc., Pittsburgh, PA, 1998.
[57] G. Schaftenaar, MOLDEN 3.4 CAOSCAMM Center, The Netherlands, 1998.
[58] A.D. Becke, Phys. Rev. A 38 (1988) 3098.
[59] J.P. Perdew, Phys. Rev. B 33 (1986) 8822.

[60] (a) C. Chang, M. Pelissier, Ph. Durand, Phys. Scr. 34 (1986) 394;
(b) J.-L. Heully, I. Lindgren, E. Lindroth, S. Lundquist, A.-M. Martensson-Pendrill, J. Phys. B 19 (1986) 2799;
(c) E. van Lenthe, E.J. Baerends, J.G. Snijders, J. Chem. Phys. 99 (1993) 4597;
(d) E. van Lenthe, E.J. Baerends, J.G. Snijders, J. Chem. Phys. 105 (1996) 6505;
(e) E. van Lenthe, R. van Leeuwen, E.J. Baerends, J.G. Snijders, Int. J. Quantum Chem. 57 (1996) 281;
(f) E. van Lenthe, A.E. Ehlers, E.J. Baerends, J. Chem. Phys. 110 (1999) 8943.
[61] J.G. Snijders, E.J. Baerends, P. Vernooijs, At. Data Nucl. Data Tables 26 (1982) 483.
[62] E.J. Baerends, D.E. Ellis, P. Ros, Chem. Phys. 2 (1973) 41.
[63] J. Krijn, E.J. Baerends, Fit Functions in the HFS-Method, Internal Report (in Dutch), Vrije Universiteit Amsterdam, The Netherlands, 1984.
[64] E.J. Baerends, J.A. Autschbach, A. Berces, C. Bo, P.M. Boerrigter, L. Cavallo, D.P. Chong, L. Deng, R.M. Dickson, D.E. Ellis, L. Fan, T.H. Fischer, C. Fonseca Guerra, S.J.A. van Gisbergen, J.A. Groeneveld, O.V. Gritsenko, M. Grüning, F.E. Harris, P. van den Hoek, H. Jacobsen, G. van Kessel, F. Kootstra, E. van Lenthe, V.P Osinga, S. Patchkovskii, P.H.T. Philipsen, ADF 2004, D. Post, C.C. Pye, W. Ravenek, P. Ros, P.R.T. Schipper, G. Schreckenbach, J.G. Snijders, M. Sola, M. Swart, D. Swerhone, G. te Velde, P. Vernooijs, L. Versluis, O. Visser, E. Wezenbeek, G. Wiesenekker, S.K. Wolff, T.K. Woo, T. Ziegler, Scientific Computing & Modelling NV, The Netherlands.
[65] (a) K. Morokuma, J. Chem. Phys. 55 (1971) 1236;
(b) K. Morokuma, Acc. Chem. Res. 10 (1977) 294.
[66] (a) T. Ziegler, A. Rauk, Theor. Chim. Acta 46 (1977) 1;
(b) T. Ziegler, A. Rauk, Inorg. Chem. 18 (1979) 1558;
(c) T. Ziegler, A. Rauk, Inorg. Chem. 18 (1979) 1755.
[67] (a) A.F. Wells, Structural Inorganic Chemistry, 5th ed., Clarendon, Oxford, 1984;
(b) L. Pauling, The Nature of the Chemical Bond, 3rd ed., Cornell University Press, Ithaca, NY, 1960.
[68] L. Pauling, The Nature of the Chemical Bond, 3rd ed., Cornell University Press, New York, 1960, p. 239, The relationship of bond order to length is given by $dn = dl - 0.71 \log n$, where n is the bond order, dl and dn are the lengths of bonds with bond order l and n, respectively.
[69] K.A. Wiberg, Tetrahedron 24 (1968) 1083.